

Fatigue Life Estimation Procedures for the Endurance of a Cardiac Valve Prosthesis: Stress/Life and Damage-Tolerant Analyses¹

R. O. Ritchie

Professor of Metallurgy,
Department of Materials Science
and Mineral Engineering,
University of California,
Berkeley, Calif. 94720

P. Lubock

Manager,
Mechanical Heart Valves,
Cardiovascular Division,
Shiley, Inc., Irvine, Calif. 92714

Projected fatigue life analyses are performed to estimate the endurance of a cardiac valve prosthesis under physiological environmental and mechanical conditions. The analyses are conducted using both the classical stress-strain/life and the fracture mechanics-based damage-tolerant approaches, and provide estimates of expected life in terms of initial flaw sizes which may pre-exist in the metal prior to the valve entering service. The damage-tolerant analysis further is supplemented by consideration of the question of "short cracks," which represents a developing area in metal fatigue research, not commonly applied to data in standard engineering design practice.

Introduction

The modern cardiac valve prosthesis must be capable of continuously regulating blood flow in "hostile" physiological environments for patient lifetimes. Under such circumstances, environmentally assisted sub-critical growth of inherent material flaws, driven by the presence of alternating stresses (approximately 38 million cycles per year) can be a principal cause of mechanical failure. In these instances, the life of the valve will be limited primarily by the process of fatigue.

The object of the current paper is to describe analytical procedures whereby the useful (fatigue) life of a prosthetic cardiac valve can be estimated using both classical stress-strain/life and damage-tolerant fatigue analyses. The valve chosen for study is the newly developed Bjork-Shiley Monostrut[®] valve, where blood flow is regulated by means of a pyrolytic carbon disk (occluder) which tilts between an inlet and outlet strut (Fig. 1). As these struts are vital to the function of the valve and are subjected to the bulk of the fatigue loading, the analysis is focused on potential growth of tiny, pre-existing flaws in these struts, particularly in the highest stressed regions at their base.

Methods of Fatigue Life Analyses

Current fatigue design and lifetime estimation procedures used in engineering practice are performed either in terms of conventional stress or strain/life analyses (also referred to as S/N curves, high/low cycle fatigue or local strain approach), which relate the total fatigue life (i.e., the number of cycles both to initiate and propagate a crack to failure) to the applied stress and/or strains, or in terms of damage-tolerant analyses,

which utilize fracture mechanics procedures to estimate solely the propagation life in terms of the number of cycles, or time, to grow the largest undetected crack to failure.

In the classical S/N approach (e.g., reference [1]) smooth-sided or notched specimens are cycled and the values of strain amplitude (ϵ_a), or applied stress amplitude (σ_a), recorded as a function of cycles to failure (N_f).² Where the resulting S/N curve is derived under conditions of zero mean stress (i.e., a stress ratio, R ,³ of -1), the predicted lives can be adjusted for a finite mean stress using conventional Goodman diagram, or equivalent, procedures. Similarly, adjustment for notches, variable amplitude loading, environment, frequency, and so forth can be made as required. In certain materials, such as steels in inert environments, a fatigue limit can be defined representing the value of the stress amplitude below which failure should not occur. In other materials, an endurance strength ($\Delta\sigma_e/2$) generally is defined representing typically the value of σ_a to yield lives in excess of 10^8 cycles. Endurance strength/fatigue limit values generally are of the order of 0.3 to 0.6 σ_u , the ultimate tensile strength (typically $\Delta\sigma_e/2 \sim \sigma_u/2$), and can be reasonably expected to be reduced by a factor of 2 or so in the presence of an active environment.

This approach to fatigue life estimation is used for the vast majority of engineering situations, such as automobiles, gears, wheels, and small components. However, since the lifetimes predicted from the laboratory-derived S/N curves represent the number of cycles both to initiate and propagate a crack, there is a potential for nonconservative predictions with this method in actual components since all structures will contain pre-existing flaws, such that the initiation life may be

¹This work was supported by the Cardiovascular Division of Shiley, Inc., Irvine, Calif.

Contributed by the Bioengineering Division for publication in the JOURNAL OF BIOMECHANICAL ENGINEERING. Manuscript received by the Bioengineering Division, May 21, 1985; revised manuscript received December 16, 1985.

²Here stress or strain amplitude, σ_a and ϵ_a , respectively, are defined as one half of the stress or strain range, i.e., $\sigma_a = \Delta\sigma/2$ and $\epsilon_a = \Delta\epsilon/2$.

³Stress ratio is defined as the ratio of minimum to maximum stress, i.e., $R = \sigma_{\min}/\sigma_{\max}$.

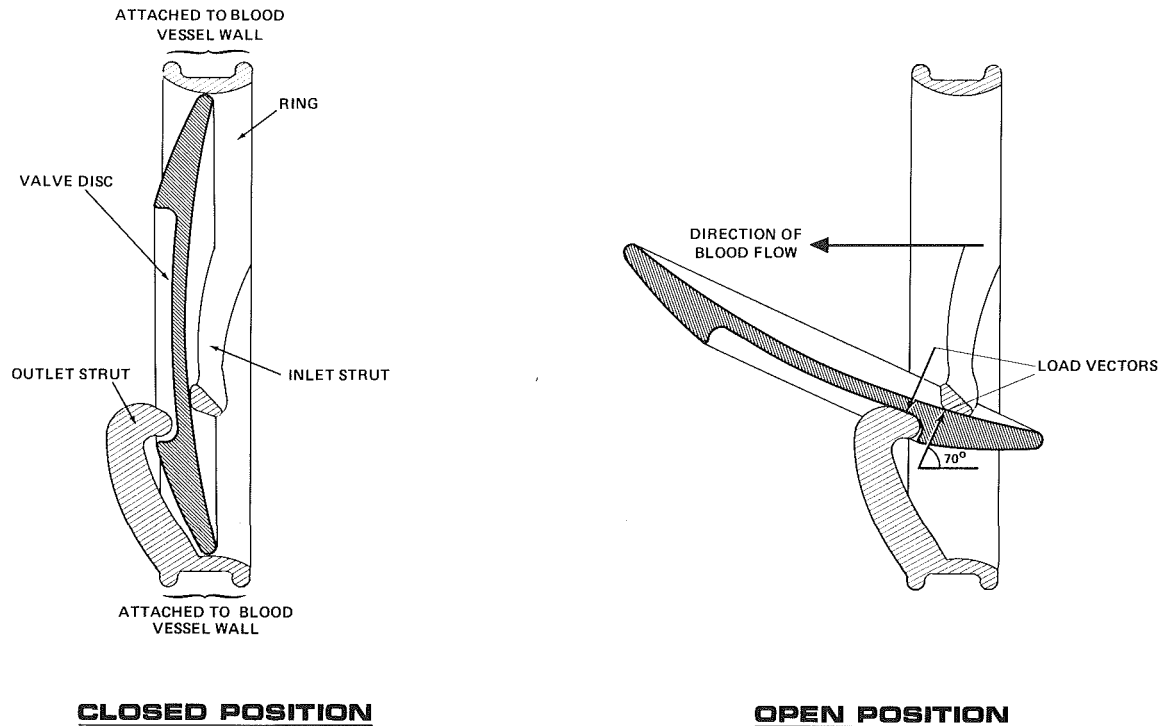


Fig. 1 Schematic illustration of the operation of the occluder in the opening and closing of the cardiac valve

negligibly small. This is particularly important in safety-critical components and in structures much larger than laboratory specimens, where the probability of significant pre-existing defects is higher. Accordingly, in these situations, the S/N approach is replaced by the so-called damage-tolerant fatigue life estimation approach, which is applied almost exclusively in the nuclear and aerospace industries (e.g., [2]). Here, the initiation life is assumed to be zero and the predicted lifetime is computed in terms of the time, or number of cycles, for the largest undetected flaw to grow to failure.

This approach utilizes a fracture mechanics characterization of crack growth where, under small-scale yielding conditions (i.e., the structure overall behaves in a linear elastic fashion), a stress intensity, K_I , can be defined which uniquely and autonomously describes the distribution of local stresses and strains in the vicinity of the crack tip in a linear elastic solid. Based on applied stress, σ , crack length, a , and geometry, K_I can be computed in any geometry from relationships of the form [3]

$$K_I = Q\sigma\sqrt{\pi a} \quad (1)$$

where Q is a geometrical factor, values of which can be determined analytically or numerically and are available for numerous cracked configurations in handbooks (e.g., reference [4]). The small-scale yielding approximation implies that the extent of local plasticity, i.e., the plastic zone size, r_y , given by $(1/2)\pi(K_I/\sigma_y)^2$ where σ_y is the yield strength [5], is small (i.e., $\sim 1/15$) compared to the in-plane dimensions of crack length and uncracked ligament. Where r_y is additionally small (i.e., $\sim 1/15$) compared to the out-of-plane thickness dimension, termed plane strain conditions, the critical value of K_I at final fracture is a material constant K_{Ic} , known as the material's fracture toughness.

Flaws subjected to stress intensities less than K_{Ic} can grow sub-critically until K_{Ic} is exceeded and failure occurs, by such mechanisms as fatigue, stress corrosion cracking, hydrogen-assisted growth and creep crack growth [6]. In general, the primary mechanism of sub-critical cracking, however, is by fatigue, generally aided by the presence of an active environment, i.e., corrosion fatigue. Under cyclic loading, where a

stress intensity can be defined both extremes of the fatigue cycle, i.e.)

$$K_{\max} = Q\sigma_{\max}\sqrt{\pi a}$$

and

$$K_{\min} = Q\sigma_{\min}\sqrt{\pi a} \quad (2)$$

the rate of crack extension per cycle (da/dN) is governed by a power law function of the range of stress intensity, $\Delta K = K_{\max} - K_{\min}$, of the form [7]:

$$da/dN = C(\Delta K)^m \quad (3)$$

where C and m are scaling constants dependent upon the material/environment system and the range of growth rates in question [8, 9]. At very low growth rates, no crack growth is apparent below the so-called threshold stress intensity range, ΔK_{TH} , where cracks (of a size larger than microstructural size-scales or the scale of local plasticity) become dormant or extend at experimentally undetectable rates [9]. The value of ΔK_{TH} can be considered effectively as a material parameter for a particular material/environment/load ratio condition, and is defined operationally by experiment as the stress intensity range at which growth rates do not exceed a certain value (usually 10^{-7} to 10^{-8} mm/cycle according to proposed ASTM standards).

Fatigue life estimation procedures using damage-tolerant analysis are used routinely in the following manner. Nondestructive evaluation (NDE) procedures, e.g., microscopy, ultrasonics, magnetic particle inspection, etc., first are used to search for incipient flaws at highly stressed locations in the given component. The initial defect size, a_0 , is either assumed or defined conservatively in terms of the resolution of this NDE procedure, i.e., as the largest undetected crack. In terms of the expected in-service stresses, an initial set of stress intensities, ΔK , K_{\max} and K_{\min} , then is computed, such that: a) if the initial $K_{\max} > K_{Ic}$, immediate fracture will occur such that the fatigue life, $N_f \rightarrow 0$; b) if the initial $\Delta K < \Delta K_{TH}$, no fatigue crack growth should occur such that $N_f \rightarrow \infty$; or c) if $\Delta K > \Delta K_{TH}$ and $K_{\max} < K_{Ic}$, crack extension will take place with the number of cycles to failure, N_f , being computed by simply integrating the crack growth

“law,” e.g., equation (3), from initial crack size (i.e., NDE limit of resolution) to final crack size (e.g., where $K_{max} = Q \sigma_{max} \sqrt{\pi a_c} = K_{Ic}$). This approach is considered inherently to be conservative primarily because of the assumption of zero initiation life and the conservative definition of the initial flaw size, a_o .

Valve Design and Mode of Loading

The basic design of valve is illustrated in Fig. 2. Both inlet and outlet struts on the valve have essentially triangular cross sections near their base with the minimum dimensions shown in Fig. 2. The valve orifice and struts are fabricated from hot-rolled bar stock of Haynes 25^{®4} cobalt-based alloy, of nominal composition shown in Table 1. Prior to machining, the alloy is given a solution anneal at 1230°C, followed by a water quench. Ambient temperature mechanical properties for this material are listed in Table 2.

Maximum surface stresses at the base of the inlet and outlet struts in the valves were estimated from pulse duplicator studies, which determine the maximum total vertical load values from measured deflections on calibrated struts under simulated service flow conditions. For peak physiological flow conditions, these maximum load values were found to be 15.7 N and 9.1 N for the inlet and outlet struts, respectively. Computation of the stresses from these loads was performed by Parks [10] with two dimensional finite element analysis using (Timoshenko) beam theory for the linear elastic deformation in each strut. The inlet strut, where the axes of the two beam sections were taken as arcs of circles, was modeled with ten three-noded quadratic displacement/rotation beam elements. Maximum computed tensile stresses were found to act at the base of the strut, at the vertex furthest away from the outlet strut (at location V in Fig. 2) during valve closing [10]. Similar numerical analysis for the outlet strut, which was modeled as a curved cantilever beam with a variable trapezoidal cross section, revealed that maximum computed nominal tensile stresses under peak physiological loading conditions act near the base on the outflow (downstream) surface during valve opening [10]. In the present analysis, we choose estimates for the nominal values of these stresses for peak physiological loading as 0 to 76 MPa in the inlet strut and 0 to 34 MPa in the outlet strut.

Stress/Life Fatigue Analysis

The stress amplitude versus life (S/N) curve for Haynes 25 alloy, based on rotating beam tests in room air and aerated 0.9 percent NaCl saline endurance strength ($\Delta\sigma_e/2$) at 18⁸ cycles at 448 MPa at $R = -1$. As both inlet and outlet struts of the cardiac valve are subjected to zero-tension nominal loading conditions, i.e., at $R = 0$, the endurance strength from Fig. 3 must be corrected to allow for the presence of a mean stress.

⁴Registered trademark of Cabot Corporation.

Table 1 Composition in weight percent of Haynes 25 alloy

C	Mn	Cr	Ni	Si	W	Fe	Co
0.1	1.5	20	10	1.0	15	3.0	balance

Table 2 Mechanical properties of Haynes 25 alloy at ambient temperatures

Elastic modulus (E)	Yield strength (σ_y)	Tensile strength (σ_u)	Elongation on 38 mm gage	Fatigue endurance strength ($\Delta\sigma_e/2$) ^(a)
(GPa)	(MPa)	(MPa)	(percent)	(MPa)
209	45B	997	64	448

^(a) $\Delta\sigma_e/2$ defined at $R = -1$ after more than 10⁸ cycles in room air.

Using the Goodman relationship, the corresponding endurance strength at $R = 0$, $\Delta\sigma_e'/2$, will be given by

$$\frac{\Delta\sigma_e'}{2} = \frac{\Delta\sigma_e}{2} \left(1 - \frac{\sigma_m}{\sigma_u}\right) \quad (4)$$

where σ_m and σ_u are the mean stress and tensile strength, respectively. For Haynes 25 alloy, allowing for a factor of 2 reduction in the endurance strength at $R = -1$ (i.e., $\Delta\sigma_e/2 = 224$ MPa) to allow conservatively for the environmental effect of physiological conditions at lower frequencies (e.g., ~ 1 Hz),⁵ this gives a value of $\Delta\sigma_e'/2$ of 183 MPa at $R = 0$, imply-

⁵The waveform used for S/N fatigue and crack propagation tests was sinusoidal. This is considered as a reasonable simulation of the physiological wave forms seen by the inlet and outlet struts, which tend to be intermediate between a sine and a square wave.

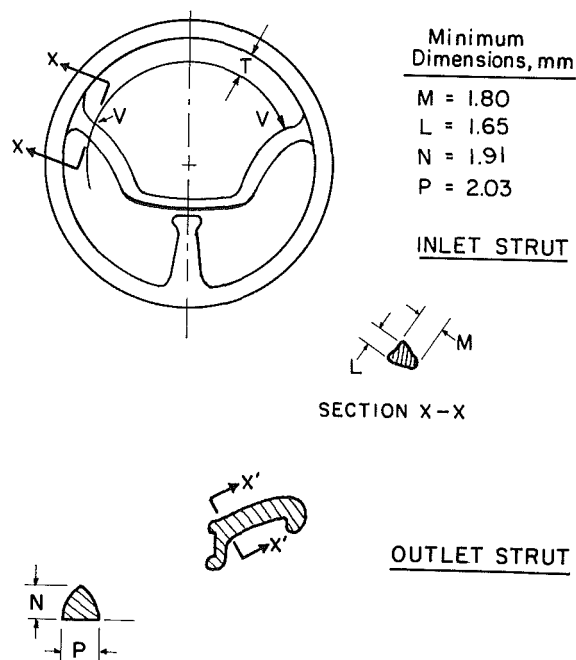


Fig. 2 Geometry of monostrut valve showing minimum dimensions and sections XX and X'X' of the inlet and outlet struts, respectively

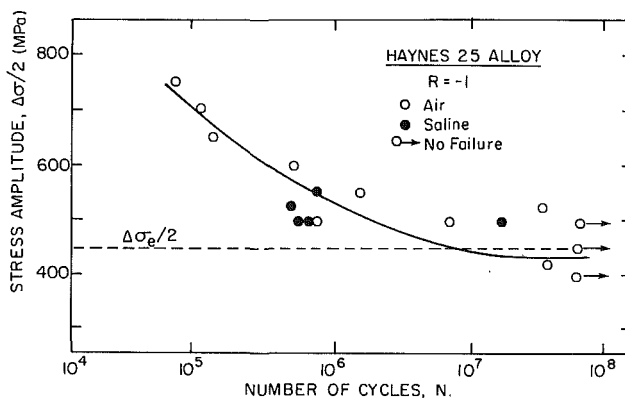


Fig. 3 Stress amplitude versus number of cycles (S/N) using rotating beam method for Haynes 25 alloy tested in air and in aerated (0.9 percent NaCl) saline solution

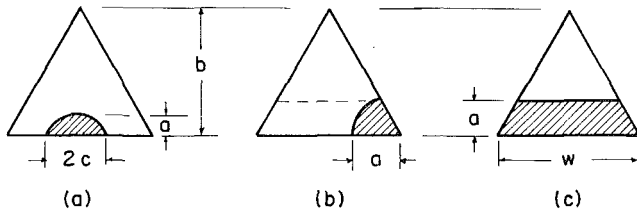


Fig. 4 Idealized crack configurations for either inlet or outlet valves showing (a) semi-elliptical half-crack, (b) corner crack, and (c) through-thickness crack. Note the characteristic cross-sectional dimensions b and w correspond to valves of M, L, N or P from Fig. 2.

ing a cyclically varying stress of ± 183 MPa about a mean of 183 MPa. Thus, the limiting stress range for no fatigue failure in 10^8 cycles under zero tension loading ($R = 0$) in this alloy will be $\Delta\sigma_e' = 366$ MPa. Comparison with the peak in-service stresses experienced at the base of the inlet and outlet struts under physiological loading conditions, i.e., 76 and 34 MPa, respectively, clearly indicates that the in-service stresses remain small, by a factor of 5 to 11, compared to the endurance strength, suggesting that failure due to fatigue crack initiation and growth should not occur in the struts during service, based on stress/life fatigue analysis.

For many engineering components, such factors of safety would be more than adequate for the assumption of no fatigue failures in less than $\sim 10^8$ cycles. However, conventional S/N analyses do not consider the existence of pre-existing flaws with the result that there is always a possibility of nonconservative predictions. In view of the safety-critical nature of a prosthetic heart valve, additional analyses were performed based on fracture mechanics where the initiation life is taken as zero and endurance is computed simply in terms of the time, or number of cycles, to propagate the largest undetected crack to failure.

Damage-Tolerant/Fracture Mechanics Analysis

The specific steps involved in the fracture mechanics analysis of the heart valve involve: (i) estimation of the variation in stress intensity (K_I) with crack size (a) for worst-case corner cracks at the base of either strut; (ii) determination of representative fatigue crack propagation (da/dN) behavior in Haynes alloy 25 under (simulated physiological conditions); (iii) computation of lifetimes in terms of an integration of the experimental da/dN data from initial to final defect sizes; (iv) consideration of the influence residual stresses; and (v) quantitative evaluation of the possible influence of the "small crack" effect where the value of the fatigue threshold may be reduced at very small crack sizes (e.g., [11]). The analysis is designed to be conservative at all stages and, with the exception of the "small crack" analysis, represents procedures used currently for engineering life prediction in safety-critical structures. The question of small cracks, conversely, is still a topic of major research interest, and, although rarely incorporated to date in general engineering design, it now is appreciated in state-of-art lifetime calculations for components such as turbine blades in jet engines [12].

Stress Intensity Solutions. The possible crack configurations for both inlet and outlet struts are shown schematically in Fig. 4. For a small elliptical half-crack, of depth a and surface $2c$, in an infinite section (Fig. 4(a)), the stress intensity K_I at maximum crack depth is given in terms of the applied stress, σ_{app} , by [4, 13]

$$K_I = \frac{\sigma_{app} \sqrt{\pi a}}{\varphi} \quad \text{for } a/b \leq 0.25 \quad (5)$$

where φ is an elliptical integral of the 2nd kind $\cong (3\pi/8) + (\pi/8)(a^2/c^2)$. Assuming a semi-circular (penny-shaped) crack with $a/2c \sim 1/2$, with $\sigma_{app}/\sigma_y \sim 0$, $\varphi = 1.57$ such that for $a/b \leq 0.25$ [13]

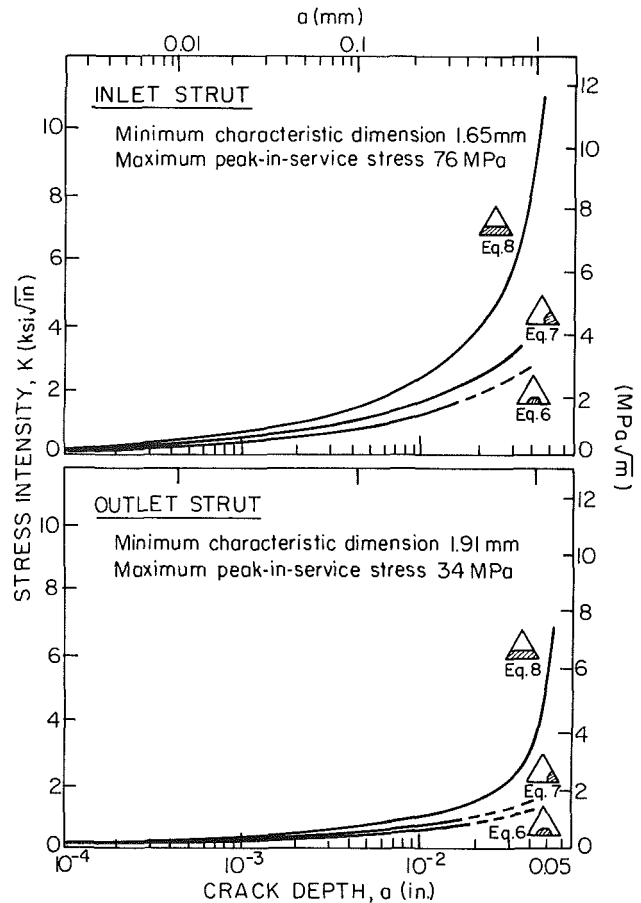


Fig. 5 Variation in stress intensity, K_I , as a function of crack depth, a , in inlet and outlet struts under physiological loading conditions (from equations (6)-(8)). Solid lines represent predictions within range of validity of K_I solutions.

$$K_I \text{ (penny-shaped half crack)} = \frac{\sigma_{app} \sqrt{\pi a}}{1.57} \approx 0.64 \sigma_{app} \sqrt{\pi a} \quad (6)$$

A more conservative approach is to consider a corner crack, of surface length a (Fig. 4(b)), where the stress intensity for an infinite section in bending has been estimated to be less than [10]

$$K_I \text{ (corner crack)} \approx 0.8 \sigma_{app} \sqrt{\pi a} \quad \text{for } a/b \leq 0.25 \quad (7a)$$

This solution remains conservative for a section of finite width provided the size of the crack is less than approximately 25 percent of the characteristic cross-sectional dimension, i.e., provided $a/b \leq 0.25$. For deeper cracks with this geometry, more recent numerical calculations [14], specifically for the present inlet strut configuration, show the stress intensity for a crack halfway through the section ($a/b = 0.5$) to be given by

$$K_I \text{ (corner crack)} \approx 0.95 \sigma_{app} \sqrt{\pi a} \quad \text{for } a/b = 0.50 \quad (7b)$$

Finally, a far more conservative approach is to consider a through-thickness crack of depth, a , and surface length equal to the entire length of the base of the section, w (Fig. 4(c)). For a finite-sized section of height, b , the K_I solution in pure bending is given by [4]

$$K_I \text{ (through-thickness crack)} \approx Q \sigma_{app} \sqrt{\pi a}, \quad \text{for } 0 < a/b < 1$$

where

$$Q \approx \sqrt{\frac{2b}{\pi a} \tan \frac{\pi a}{2b} \left[\frac{0.923 + 0.199 \left(1 - \sin \frac{\pi a}{2b}\right)^4}{\cos \frac{\pi a}{2b}} \right]} \quad (8)$$

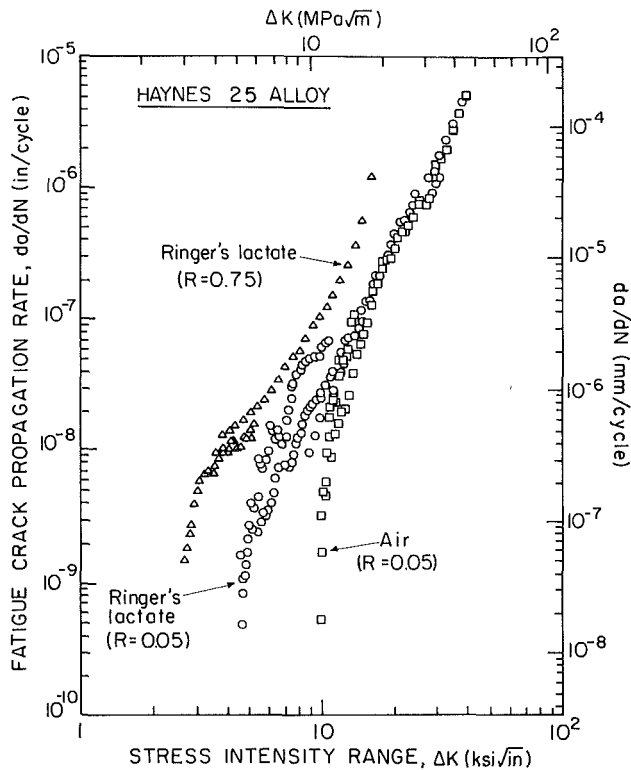


Fig. 6 Variation in fatigue crack propagation rates (da/dN) as a function of stress intensity range (ΔK) for Haynes alloy 25, tested at $R = 0.05$ and 0.75 in air and Ringer's lactate solution at 37°C (after [15])

A comparison of the resulting stress intensity K_I values as a function of crack depth, a , for the three solutions (equations (6)–(8)) as applied to both the inlet and outlet struts, is shown in Fig. 5. In each case, worst-case computations for the respective inlet and outlet struts are performed for the maximum peak in-service stresses of 76 MPa and 34 MPa, at minimum characteristic dimensions of 1.65 and 1.91 mm.

The results in Fig. 5 indicate that for initial crack depths of 25 percent of the strut dimensions (i.e., crack depths of 413 μm and 476 μm in the inlet and outlet struts, respectively), where all solutions are within their range of validity, the initial stress intensity K_I levels do not exceed 3.3 MPa $\sqrt{\text{m}}$ in the inlet strut and 1.5 MPa $\sqrt{\text{m}}$ in the outlet strut.

In terms of NDE procedures for crack detection, the relevant dimension on crack size is the surface crack length. From service experience, penny-shaped cracks are the most probable. However, stress intensities developed ahead of such cracks are lower than for corner cracks at corresponding crack depths (i.e., ~ 20 percent lower at $a/b = 0.25$). Accordingly, for conservatism, equation (7) for the corner crack is considered as the optimum solution for both struts in terms of detectable surface crack lengths and is used in the remainder of the analysis. The through-thickness crack solution (equation (8)) is not used further, as it already assumes a surface crack length equal to the full section thickness, i.e., $a \sim 1650$ to $2000 \mu\text{m}$.

Figure 5 indicates that for physiological loading conditions, the largest stress intensity (from equation (7)) in either the inlet or outlet struts does not exceed $K_I = 2 \text{ MPa}\sqrt{\text{m}}$ for an initial flaw of surface crack length less than 25 percent of the minimum characteristic dimension of the strut, i.e., for flaws of surface length less than $400 \mu\text{m}$. Moreover, in the more heavily stressed inlet strut, where equation (7) is valid to $a/b = 0.5$, the initial stress intensity does not exceed $3.7 \text{ MPa}\sqrt{\text{m}}$ for a crack halfway through the section (i.e., for $a \sim 825 \mu\text{m}$).

Fatigue Crack Propagation Data. Fatigue crack propagation rate (da/dN) data, as a function of stress intensity range,

Table 3 Fatigue crack growth threshold data for Haynes 25 alloy

Load ratio R (K_{\min}/K_{\max})	Environment	Threshold ΔK_{TH} (MPa $\sqrt{\text{m}}$)
0.05	37°C Ringer's solution	4.67
0.05	37°C Ringer's solution	4.51
0.75	37°C Ringer's solution	2.58
0.05	22°C room air	10.57

ΔK , were obtained for Haynes alloy 25 in simulated physiological environment [15]. Crack growth rates were monitored using compliance techniques over an extremely wide range of da/dN , namely over 5 orders of magnitude down to near-threshold levels below 10^{-7} mm/cycle. Values of the fatigue threshold (ΔK_{TH}) also were determined, using the most conservative of the proposed ASTM definitions, i.e., at $da/dN = 10^{-8}$ mm/cycle.

To simulate the actual heart valve material condition, specimens of the standard compact tension $C(T)$ type were machined from regular 29-mm-dia Haynes Alloy 25 rod to a thickness of 2.5 mm and a width of 23 mm. To simulate physiological conditions, tests were performed at 37°C in lactated Ringer's solution using sinusoidal frequencies of 30 Hz down to ΔK_{TH} values and 30 and 3 Hz⁶ at the threshold. Stress ratios of 0.05 and 0.75 were used to simulate approximately nominal loading conditions and conditions with a large tensile mean (or residual) stress, respectively.

Tests at $R = 0.05$ in Ringer's solution were repeated twice, and, for comparison, an additional test was performed at $R = 0.05$ in room temperature air (46 percent relative humidity). The results [15] of all tests are shown in Fig. 6, and threshold ΔK_{TH} values are listed in Table 3.

Using the most conservative approach, the variation in da/dN with ΔK was estimated quantitatively by taking a regression fit to the near-threshold data below 10^{-7} mm/cycle. Thus, for the heart valve material under simulated physiological environment with nominal zero-tension loading conditions ($R = 0$), the fatigue crack growth behavior can be described, in units of MPa $\sqrt{\text{m}}$ and m/cycle, by

$$da/dN = (7.10 \times 10^{-20}) \Delta K^{12.2}$$

with

$$\Delta K_{\text{TH}} \sim 4.5 \text{ MPa}\sqrt{\text{m}} \quad (9)$$

Lifetime Calculations. A comparison of the fatigue threshold value ($\Delta K_{\text{TH}} = 4.5 \text{ MPa}\sqrt{\text{m}}$ for behavior in simulated physiological environment/loading conditions) with the computations in Fig. 5 (specifically from equation (7)) showing the initial ΔK values (developed for physiological loading) as a function of initial surface crack size, a_0 , indicates that for both inlet and outlet struts, ΔK will be less than ΔK_{TH} for all crack sizes less than 50 percent of the cross-sectional dimension of the strut. Thus, provided NDE procedures can reliably detect all cracks in excess of a surface length of roughly $800 \mu\text{m}$, initial ΔK values at peak in-service loading will be less than the threshold ΔK_{TH} . If NDE can detect cracks down to $400 \mu\text{m}$, initial ΔK values will be better than a factor of 2 less than ΔK_{TH} . This implies that fatigue crack propagation leading to failure during a service life would be unlikely, if all incipient surface flaws larger than 400 to $800 \mu\text{m}$ in size are detected.

A more conservative approach is to disregard the concept of an absolute threshold and assume that growth rates do not terminate but continue at very low ΔK values to vanishingly small levels. With this procedure, a finite life can be predicted by integrating the relevant near-threshold crack growth "law" between limits of initial crack size a_0 (i.e., the limit of resolution of the NDE procedure) to final failure. Thus using equation (1) with conservative values of m and C measured for this

⁶No effect of frequency between 3 and 30 Hz was detected for growth rates at near-threshold levels.

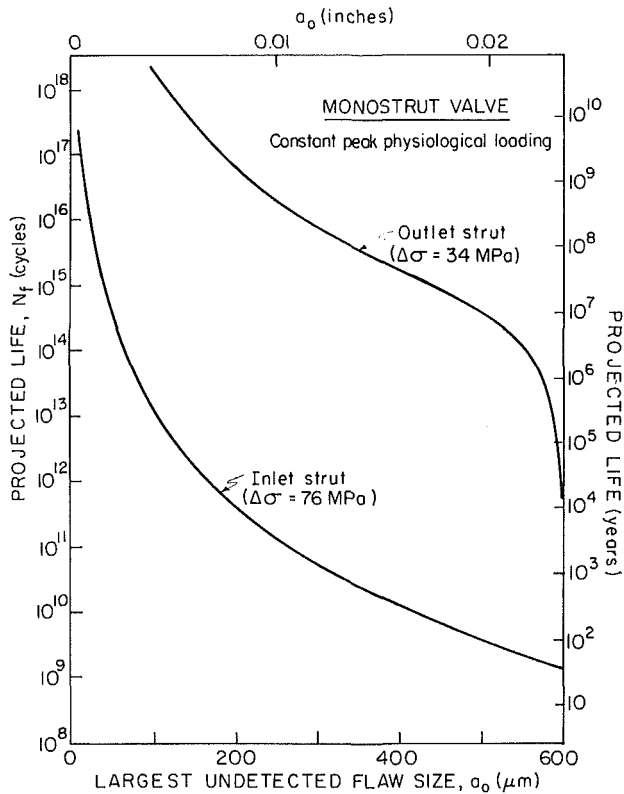


Fig. 7 Damage-tolerant projections of the fatigue lifetime of the valve (N_f) as a function of the largest undetected flaw size (a_o) in the inlet and outlet struts for continuous physiological loading

alloy (equation (9)), and the appropriate K_I solution (equation (7))

$$da/dN = C(\Delta K)^m$$

and

$$K_I = Q\sigma\sqrt{\pi a}$$

where

$$Q = 0.8-0.95, C = 7.10 \times 10^{-20} \text{ and } m = 12.2$$

yields

$$da/dN = C(Q\Delta\sigma)^m \pi^{m/2} a^{m/2} \quad (9)$$

Rearranging and integrating between initial and final crack sizes, a_o and a_f , respectively, to give the propagation life, N_f , yields

$$\int_{a_o}^{a_f} \frac{da}{a^{m/2}} = C(Q\Delta\sigma)^m \pi^{m/2} \int_0^{N_f} dN \quad (10)$$

such that

$$N_f = \frac{2}{(m-2)C(Q\Delta\sigma)^m \pi^{m/2}} \left[\frac{1}{a_o^{(m-2)/2}} - \frac{1}{a_f^{(m-2)/2}} \right]$$

$$= \frac{2.58 \times 10^{15}}{(Q\Delta\sigma)^{12.2}} \left[\frac{1}{a_o^{5.1}} - \frac{1}{a_f^{5.1}} \right] \quad (11)$$

For the assumed in-service loading values of $\Delta\sigma$ of 76 MPa and 34 MPa for the inlet and outlet struts, respectively, equation (11) is evaluated to give the estimated fatigue lifetime N_f as a function of initial flow size (a_o). Failure is defined conservatively as a surface crack size of $a_f = 890 \mu\text{m}$, i.e., at approximately 54 percent of the cross-sectional dimension, in the inlet strut and as $a_f = 600 \mu\text{m}$ in the outlet strut, as dictated by the validity of equation (7). These projected lifetimes are plot-

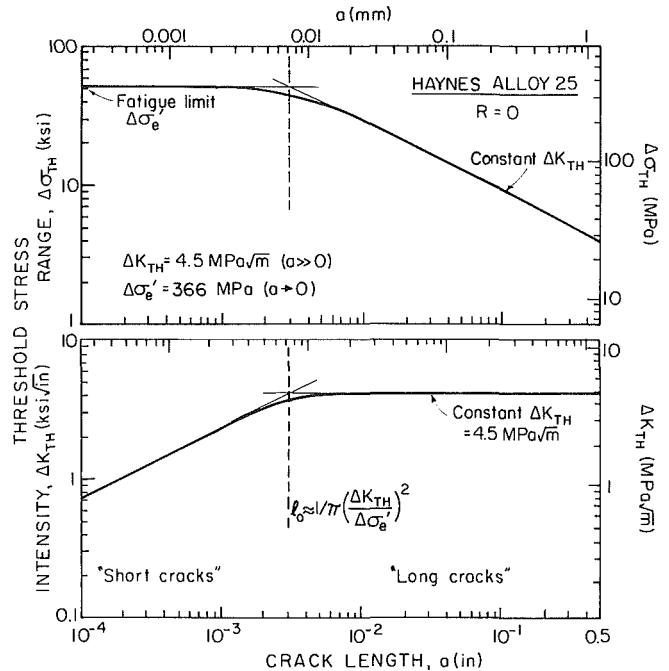


Fig. 8 Variation with crack size (a) with threshold stress range ($\Delta\sigma_{TH}$) and threshold stress intensity range (ΔK_{TH}) for no crack growth. Predictions, based on equations (13)-(16), for Haynes alloy 25 ($\sigma_y = 458 \text{ MPa}$) at $R \sim 0$, where $\Delta K_{TH} = 4.5 \text{ MPa}\sqrt{\text{m}}$ from long crack tests ($a > l_o$) and $\Delta\sigma_e' = 366 \text{ MPa}$ estimated from smooth bar endurance tests. Threshold condition is one of a constant stress intensity (ΔK_{TH}) at long crack sizes ($a > l_o$) and a constant stress (\sim fatigue limit $\Delta\sigma_e$) at short crack sizes ($a \leq l_o$).

ted in Fig. 7 assuming approximately 38×10^6 cycles of loading per year. It is clear that the life of the valve is a strong function of the resolution of the prior NDE inspection technique, i.e., of the largest undetected flaw size. Based on these computations, the damage-tolerant analysis predicts that, for continuous peak in-service physiological loading of 0 to 76 MPa in the inlet strut and 0 to 34 MPa in the outlet strut in simulated physiological environments, it should take in excess of 3×10^9 cycle (i.e., approximately 90 yr) to grow a crack in either strut to failure, provided all initial cracks, of surface lengths above $500 \mu\text{m}$, are detected by NDE prior to entering service.

Influence of Residual Stresses. Residual stresses present in the part effectively will impart an additional mean stress on the nominal zero-tension ($R = 0$) loading conditions. In general, compressive residual stresses, which reduce the load ratio R , are beneficial in increasing fatigue life since the compression opposes crack opening and thus reduces both crack initiation and growth. Tensile residual stresses, which raise R , conversely are detrimental to life as they can increase growth rates and decrease threshold ΔK_{TH} values, as shown for Haynes alloy 25 in Fig. 6.

With the present heart valve, residual stresses in the inlet strut should be negligible. However, during the occluder insertion process, which involves a sequence of three displacement-controlled plastic bending operations, the outlet strut is intentionally left with residual stresses. On the outflow (downstream) side at the base, where the highest tensile stresses are applied during service, these residual stresses are compressive. Numerical calculations [10] suggest that at the surface these residual compressive stresses could be as high as 240 MPa, indicating that the foregoing damage-tolerant analysis for the outlet strut should be highly conservative. Residual stresses are correspondingly tensile on the inflow (upstream) side of the outlet strut; but this region sees only applied compressive stresses during service.

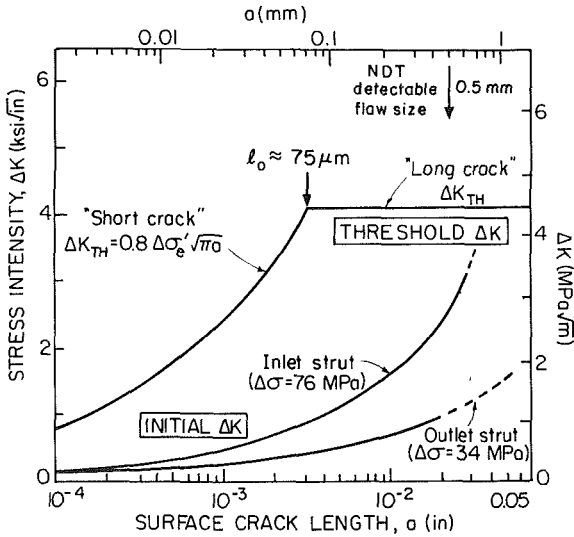


Fig. 9 Variation of threshold stress intensity, ΔK_{TH} , for both "long" and "short" cracks, and initial stress intensity, ΔK , for physiological loading, as a function of surface crack length, a , for valve. Note how for all crack sizes, the initial stress intensity is well below ΔK_{TH} , provided NDE rejects components containing flaws larger than 500 μm .

Short Crack Analysis

Recent studies in fatigue research have questioned the uniqueness of growth rates and particularly the value of the fatigue threshold in the presence of so-called "short cracks," where the term "short cracks" refers to flaws small compared to the scale of microstructure and/or scale of local plasticity, or to flaws which simply are physically small, e.g., less than 0.5 mm long [11, 16–19]. The fracture mechanics analysis of such short flaws is still the object of much research (for a recent review, see reference [11]), and thus rarely is incorporated in general engineering design of lifetime calculations. However, in view of the safety critical aspect of the current application, some consideration of the "short crack" question is warranted.

The short crack question can be posed with reference to Fig. 8 which can be viewed as a schematic variation of the threshold conditions, i.e., the threshold stress range $\Delta\sigma_{TH}$ and threshold stress intensity range ΔK_{TH} for no fatigue failure, as a function of crack size a . The bounds of this variation represent the well-known S/N and damage-tolerant procedures already discussed; i.e., for smooth samples with vanishingly small cracks, the limiting threshold condition from S/N analysis is to maintain a stress range below the fatigue limit or endurance strength, $\Delta\sigma < \Delta\sigma_e$, whereas for samples containing "long cracks," the limiting threshold condition from damage-tolerant analysis is to maintain a stress intensity range below the fatigue threshold, $\Delta K < \Delta K_{TH}$. Thus, unification of the two concepts for all crack sizes naturally demands: (i) the fatigue limit or endurance strength, $\Delta\sigma_e$ (which is a "material constant" for smooth samples) to be reduced in the presence of larger pre-existing flaws; and (ii) the fatigue threshold stress intensity, ΔK_{TH} (which is a "material constant" for samples containing "long cracks") to be reduced in the presence of smaller pre-existing flaws. The transition crack size, l_o , representing an approximate estimate of what constitutes a short crack, is thus given by [16]

$$l_o \approx \frac{1}{\pi} \left(\frac{\Delta K_{TH}}{\Delta\sigma_e} \right)^2 \quad (13)$$

where both ΔK_{TH} and $\Delta\sigma_e$ are corrected for the same stress ratio. Accordingly, it has been proposed that, given the measured values of ΔK_{TH} and $\Delta\sigma_e$, an indication of the variation in threshold stress intensity range with crack size can be deduced empirically from [16]

$$\Delta K_{TH}(a) \approx Q \Delta\sigma_{TH} \sqrt{\pi(a + l_o)} \quad (14)$$

where Q is the geometry factor in the $K_I(a)$ relationship (e.g., equation (1)).

Applying these considerations to the current fatigue analysis of the inlet and outlet struts suggests that, in general, this question of short flaws should not be a major problem, since for physiological conditions, it already has been established that the S/N analysis on smooth samples shows $\Delta\sigma < \Delta\sigma_e$ and that the damage-tolerant analysis on "long" cracked samples shows $\Delta K < \Delta K_{TH}$. However, in the context of the fracture mechanics/damage-tolerant analysis of the struts, it is instructive to estimate the possible reduction, at small crack sizes, of threshold ΔK_{TH} values from that measured for "long cracks" on standard test pieces (Fig. 6, Table 3).

Using the lower-bound measured value of the "long crack" threshold in Ringer's lactate solution of $\Delta K_{TH} = 4.5 \text{ MPa}\sqrt{\text{m}}$ at $R = 0$, and the corresponding endurance strength at 10^8 cycles of $\Delta\sigma_e' = 366 \text{ MPa}$ similarly at $R = 0$ for Haynes alloy 25, an estimate of the transition crack size l_o for the corner crack geometry is given by

$$l_o \approx \frac{1}{\pi} \left(\frac{\Delta K_{TH}}{0.8 \Delta\sigma_e'} \right)^2 \sim 75 \mu\text{m} \quad (15)$$

This implies that, in terms of the damage-tolerant fatigue analysis, values of ΔK_{TH} may be expected to be reduced progressively at crack sizes below 75 μm . However, since the initial stress intensity range ΔK developed for physiological loads also will be decreased progressively with decreasing crack size, to ensure the same margin of safety with respect to limiting fatigue failures, the value of ΔK must be shown to remain below ΔK_{TH} values for crack sizes less than $a = 75 \mu\text{m}$.

Although there is no universally accepted procedure to date for estimating, or even experimentally measuring, this variation in threshold ΔK_{TH} with crack size [11], the foregoing approach predicts the values of ΔK_{TH} at short crack sizes to be given by

$$\begin{aligned} \Delta K_{TH}(a) &\sim 0.8 \Delta\sigma_e' \sqrt{\pi a} \quad \text{for } a < l_o \sim 75 \mu\text{m} \\ &\sim 4.5 \text{ MPa}\sqrt{\text{m}} \quad \text{for } a > l_o \sim 75 \mu\text{m} \end{aligned} \quad (16)$$

where $\Delta\sigma_e'$ is estimated conservatively at 366 MPa for $R = 0$. The resulting predictions of ΔK_{TH} and the initial stress intensity ranges, developed for physiological loads in the inlet and outlet struts, are shown in Fig. 9. These results still indicate that ΔK should remain less than ΔK_{TH} at all cracks sizes below 50 percent of the strut dimensions. Thus, despite that potential decay in threshold ΔK_{TH} values at very small crack sizes, the original conclusions of the damage-tolerant fatigue analysis still apply; i.e., that, since $\Delta K < \Delta K_{TH}$ (i.e., $da/dN < 10^{-8} \text{ mm/cycle}$), failure from fatigue crack propagation at $R \sim 0$ in both inlet and outlet struts is unlikely, provided cracks of a size in excess of 500 μm are detected prior to the valve entering service.

Summary

Both classical stress-life (S/N) and fracture mechanics-based damage-tolerant analyses for the prediction of the fatigue life of a human cardiac valve prosthesis have been described under assumed peak physiological loading conditions. Based on stress/life and crack growth rate data for Haynes alloy 25, measured in saline or Ringer's lactate solution, the analyses provide conservative estimates of the fatigue life in terms of the size of the largest undetected flaw following final nondestructive evaluation (NDE). The question of "small cracks" and their influence in promoting accelerated growth rate behavior in the near-threshold regime additionally is considered. It is found that acceptable levels of fatigue life are obtained under worst-case conditions provided that all incipient flaws larger than 500 μm are detected by NDE inspection prior to the valve entering service.

Acknowledgments

This work was supported by the Cardiovascular Division of Shiley Incorporated. Thanks are due to Drs. J. K. Donald, D. M. Parks, and R. M. Pelloux for their critical input to this study.

References

- 1 Mitchell, M. R., "Fundamentals of Modern Fatigue Analysis for Design," *Fatigue and Microstructure*, American Society for Metals, Metals Park, Ohio, 1979, pp. 385-466.
- 2 Fine, M. E., and Ritchie, R. O., "Fatigue-Crack Initiation and Near-Threshold Crack Growth," *Fatigue and Microstructure*, American Society for Metals, Metals Park, Ohio, 1979, pp. 245-278.
- 3 Irwin, G. R., *Fracture, Handbuch der Physik*, Springer, Berlin, Vol. 6, 1958, pp. 551-590.
- 4 Tada, H., Paris, P. C., and Irwin, G. R., *The Stress Analysis of Cracks Handbook*, Del Research Corp., St. Louis, Mo., 1973.
- 5 Rice, J. R., "Mechanics of Crack Tip Deformation and Extension by Fatigue," *Fatigue Crack Propagation*, ASTM STP 415, American Society for Testing and Materials, Philadelphia, Pa., 1976, pp. 247-309.
- 6 Johnson, H. H., and Paris, P. C., "Sub-Critical Flaw Growth," *Engineering Fracture Mechanics*, Vol. 1, 1968, pp. 3-45.
- 7 Paris, P. C., and Erdogan, F., "A Critical Analysis of Crack Propagation Laws," *ASME Journal of Basic Engineering*, Vol. 85, 1963, pp. 528-533.
- 8 Lindley, T. C., Richards, C. E., and Ritchie, R. O., "The Mechanics and Mechanisms of Fatigue Crack Growth in Metals: A Review," *Metallurgica and Metal Forming*, Vol. 43, 1976, pp. 268-280.
- 9 Ritchie, R. O., "Near-Threshold Fatigue Crack Propagation in Steels," *International Metals Reviews*, Vol. 20, 1979, pp. 205-230.
- 10 Parks, D. M., and Synder, M. D., "Stress Analysis of Shiley Monostrut Valves," Final Report to Shiley Inc., D. M. Parks, Swampscott, Mass., 1984.
- 11 Suresh, S., and Ritchie, R. O., "The Propagation of Short Fatigue Cracks," *International Metals Reviews*, Vol. 29, 1984, pp. 445-476.
- 12 Jeal, R. H., "The Relationship between Fatigue Modelling and Component Integrity," *Fatigue '84, Proceeding 2nd International Conference on Fatigue and Fatigue Thresholds*, eds., C. J. Beevers, Vol. 3, EMAS Ltd., Warley, England, 1985, pp. 1865-1879.
- 13 Broek, D., *Elementary Engineering Fracture Mechanics*, 3rd Edition, Sijthoff, 1981.
- 14 Parks, D. M., "Stress Intensity Factor Calibration for Inlet Strut of 29 mm Shiley Monostrut Replacement Heart Valves," Report to Shiley Inc., D. M. Parks, Swampscott, Mass., Apr. 1985.
- 15 Donald, J. K., "Fatigue Crack Growth Rate Testing of Haynes 25 Material Using Compliance Measurement Technique," Final Report to Shiley Inc., Professional Service Group, Hellertown, Pa., 1984.
- 16 El Haddad, M. H., Smith, K. N., and Topper, T. H., "Fatigue Crack Propagation of Short Cracks," *ASME Journal of Engineering Materials and Technology*, Vol. 101, 1979, pp. 42-46.
- 17 Taylor, D., and Knott, J. F., "Fatigue Crack Propagation Behavior of Short Cracks; The Effect of Microstructure," *Fatigue of Engineering Materials and Structures*, Vol. 4, 1981, pp. 147-155.
- 18 Ritchie, R. O., and Suresh, S., "The Fracture Mechanics Similitude Concept: Questions Concerning its Application to the Behavior of Short Fatigue Cracks," *Materials Science and Engineering*, Vol. 57, 1983, pp. L27-L30.
- 19 Lankford, J., "The Influence of Microstructure on the Growth of Small Fatigue Cracks," *Fatigue and Fracture of Engineering Materials and Structures*, Vol. 8, 1985, pp. 161-175.